

Disorder-induced scattering loss of line-defect waveguides in photonic crystal slabs

E. Kuramochi,^{1,*} M. Notomi,¹ S. Hughes,^{1,†} A. Shinya,¹ T. Watanabe,² and L. Ramunno³

¹NTT Basic Research Laboratories, NTT Corporation, 3-1 Morinosato Wakamiya, Atsugi, Kanagawa 243-0198, Japan

²NTT Microsystem Integration Laboratories, NTT Corporation, 3-1 Morinosato Wakamiya, Atsugi, Kanagawa 243-0198, Japan

³Department of Physics, University of Ottawa, Ottawa, Ontario, Canada

(Received 12 September 2005; published 31 October 2005)

Detailed propagation loss spectrum measurements for line-defect waveguides in silicon photonic crystal slabs are presented, which show record low loss values (5 dB/cm) and complicated frequency dependence. We quantitatively analyze the origin of the loss spectrum shape using a photon Green function theory and obtain a very good agreement, thus providing an explanation of the complex physical mechanisms responsible for the observed propagation loss. In particular, we demonstrate the influence of out-plane, backward, intermode, and in-plane scattering processes on the observed loss spectra, induced by the structural disorder that occurs during fabrication, and highlight the importance of backward and intermode scattering in these waveguides.

DOI: [10.1103/PhysRevB.72.161318](https://doi.org/10.1103/PhysRevB.72.161318)

PACS number(s): 81.16.Nd, 42.70.Qs, 42.25.Fx, 42.79.Gn

Line defects in a two-dimensional (2D) photonic-crystal-slab (PCS) with photonic-band gaps (PBGs) can function as ultrasmall and tightly confined optical waveguides.¹ Theory and experiment show that PCS waveguides possess several unique features.¹⁻³ However, PCS waveguides are expected to yield a larger propagation loss because of their complicated shapes. Early investigations reported losses greater than 100 dB/cm,⁴ and somewhat later we reported a value of 60 dB/cm.^{5,6} Recently, several studies have reported a significant loss reduction.⁷⁻⁹ In spite of recent technological advances, there has been very little physics investigation of the PCS waveguide loss mechanisms—which are expected to be fundamentally different from that of conventional waveguides.¹⁰ It is generally believed that loss scales as $1/v_g$ (group velocity),¹¹ but its relevance has not yet been clarified. In this Rapid Communication, we provide detailed propagation loss measurements of record low loss PBG waveguides fabricated in Si PCSs. Moreover, we undertake an explanation of the physical mechanisms in order to explain the observed loss spectra by comparing with a recent theoretical model based on a photon Green function tensor (GFT) approach.¹² We clarify that the propagation loss reflects underlying physics relating to several different scattering mechanisms, and that loss scaling is in fact significantly more complicated than a simple v_g -scaling expectation.

Electron beam lithography is employed to fabricate Si air-cladding PCSs with hexagonal lattice air holes and a large PBG in the TE polarization ($\mathbf{E} \parallel 2\text{D}$ plane) from silicon-on-insulator wafers.³ We made a single-missing-hole line defect waveguide (W1.0) and a width-reduced waveguide (W0.7), whose width was 70% that of W1.0.^{3,5,6} The lattice period a and hole radius r are 430 nm and $0.25a$ for W1 and 400 nm and $0.275a$ for W0.7. Figure 1(a) shows scanning electron microscope (SEM) images of our PCS structure. The dry-etched sidewalls were almost vertical. The in-plane sidewall roughness σ (which is the rms of the deviation from an ideal sidewall shape) was determined to be 3 nm for our samples as a result of the statistical analysis of SEM images. This ultrasmall roughness was due to the high spatial resolution (1 nm) and small proximity effects for our electron-beam lithography process.

The TE polarization transmission spectra for different length waveguides on a single chip were measured [see Fig. 1(b)]. Figure 2(a) shows the transmittance spectra of W1.0 waveguides of different lengths. The propagation loss at each ω was deduced from the exponential fit of the length dependence of the transmittance intensity^{7,11} considering Si waveguide loss (~ 0.1 dB/cm). The accuracy of this method was mainly determined by the coupling error (± 0.25 dB in our setup). Figures 2(b) and 2(c) display the deduced loss spectra for the W1.0 and W0.7 waveguides. The lowest loss value is ~ 5 dB/cm for W1.0, which is the lowest ever reported for these PCS waveguides. Note that the bandwidth of the low loss region (loss < 10 dB/cm) is ~ 50 nm, which is significantly larger than previous reports.

Interestingly, the loss spectra in Figs. 2(b) and 2(c) show a rich and complex ω dependence quite unlike that of regular waveguides. We next focus on this exotic loss spectrum shape, in order to yield insight into the physical mechanisms responsible for the observed loss. First, we consider the dispersion curve for the waveguide modes. The dispersion curves for W1.0 and W0.7 waveguides are shown in Figs. 1(c) and 1(d). Both waveguides have clear cutoff frequencies at the mode-gap edge (ω_{ge}), from which light propagation is inhibited. Experimentally, we can easily determine the mode-gap position by looking at the transmission drop for very short waveguides. The shaded area in Figs. 2(b) and 2(c) shows the experimentally determined mode-gap cutoff region. The position of the shaded area coincides well with the theoretically calculated ω_{ge} . Another issue we have to consider is the light-line cutoff ω_{ll} , above which the mode experiences a large intrinsic radiation loss into the cladding. While ω_{ge} and ω_{ll} explain the observed transmission window width, but they tell us nothing about the loss spectrum shape inside the window. Theoretically, the modes between the two cutoffs are *lossless* for ideal PCS waveguides with perfect translational invariance. Any propagation loss that does occur in this region is *extrinsic* scattering loss due to fabrication structural disorder, which destroys the translational invariance.

Extrinsic propagation loss can be treated as an electro-

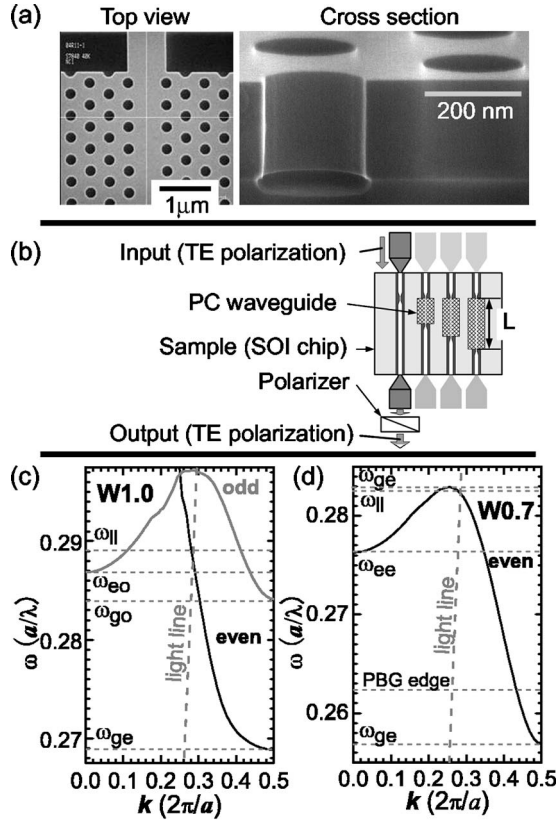


FIG. 1. PCS waveguides and their dispersion curves. (a) SEM images of the W1.0 PCS waveguide structure. (b) Schematic of the chip design used for the loss measurement. (c), (d) Calculated dispersion curves for waveguides (c) W1.0 and (d) W0.7. k (x axis) is a normalized wave number and ω (y axis) is the normalized frequency. The frequencies are ω_{ge} , ω_{go} : the mode-gap edge of the even/odd mode; ω_{ee} , ω_{eo} : the edge of the doubled even/odd mode; ω_{ll} : even mode crosses light line of air.

magnetic scattering problem. Here we examine it within a second-order Born approximation using a recently developed photon-Green function-tensor (GFT) solution by which the effect of structural disorder can be incorporated in a very straightforward manner.¹³ With the GFT method, the scattering loss $L(\omega)$ is expressed as

$$L(\omega) = \frac{a\omega}{v_g} \int \int d\mathbf{r}d\mathbf{r}' \Delta\varepsilon(\mathbf{r})\Delta\varepsilon(\mathbf{r}') \times \text{Im}\{\mathbf{e}_k^*(\mathbf{r})\mathbf{G}(\mathbf{r},\mathbf{r}';\omega)\mathbf{e}_k(\mathbf{r}')e^{ik(x-x')}\}, \quad (1)$$

with \mathbf{e}_k the normalized Bloch mode, \mathbf{G} the total GFT for PCS *without disorder*, and $\Delta\varepsilon$ describes the spatially dependent structural disorder, which is the source of the scattering. Evidently, the loss roughly scales as the product of $1/v_g$ and $\text{Im}[G]$. Thus, if $\text{Im}[G]$ is constant, $L(\omega)$ would scale as $1/v_g$ as expected. Let us briefly consider the meaning of $\text{Im}[G]$. Intuitively, this part represents the local photon density of states (LDOS) of the final state of the scattering process. With normal waveguides, the dominant contribution to the LDOS is from the effective medium radiation modes [in three-dimensional (3D) free space], that is almost constant

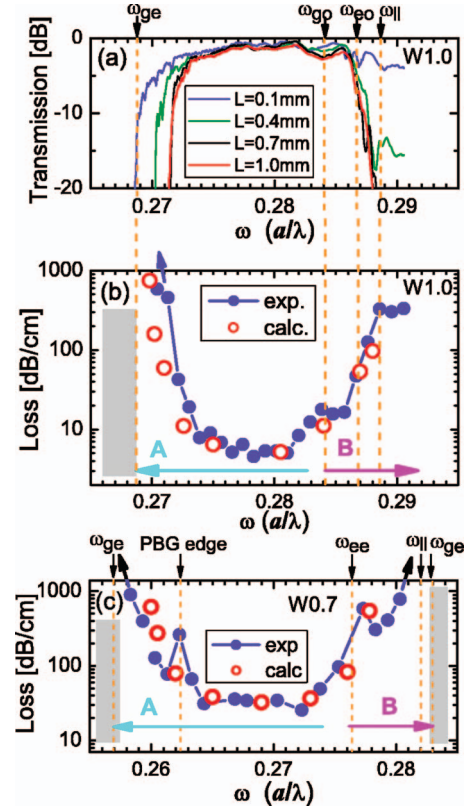


FIG. 2. (Color) Transmission and loss spectra. (a) The transmission spectrum for the W1.0 waveguides with different lengths (0.1, 0.4, 0.7, and 1.0 mm). (b) The loss spectrum for the W1.0 waveguides. (c) The loss spectrum for W0.7 waveguides. The solid circles and lines are measured data. The theoretical loss spectra obtained by the GFT method are also shown by open circles. The characteristic frequencies determined from Figs. 1(c) and 1(d) are shown by arrows.

within the spectrum. However, it is not so simple with PCS waveguides. In Fig. 3(a), we plot the product of the measured loss and calculated v_g for W1.0. Apparently a simple v_g -scaling picture does not explain the complicated $L(\omega)$. In Fig. 4, we show the calculated $\text{Im}[G]$ at $\mathbf{r}=\mathbf{r}'$ on an edge of the hole nearest the waveguide, which is a typical large source of scattering loss. The G tensors were obtained numerically using a finite-difference time-domain method, that demonstrate that $\text{Im}[G]$ is far from constant. Consequently

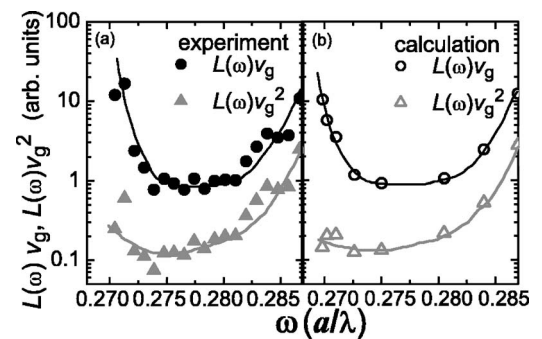


FIG. 3. $L(\omega)v_g$ and $L(\omega)v_g^2$ plot [$L(\omega)$: loss] of W1.0 waveguides for (a) measured data and (b) calculated data.

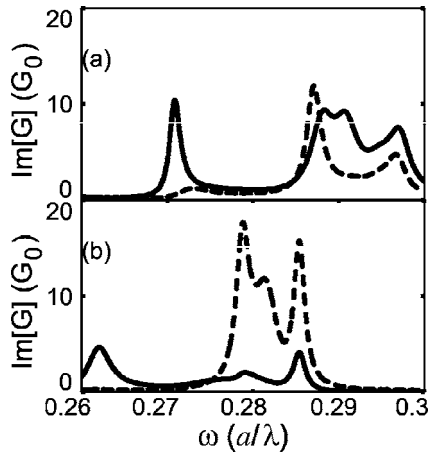


FIG. 4. Calculated $\text{Im}[G]$ spectra. $\text{Im}[G_{xx}]$ (solid curve) and $\text{Im}[G_{yy}]$ (dashed curve) elements for waveguides at $\mathbf{r}=\mathbf{r}'$ on an edge of the hole nearest to the waveguide (a) W1.0 and (b) W0.7. The units are scaled to the free-space value G_0 .

we observe fairly complicated loss spectra that do not simply scale with v_g , and we next investigate the underlying physical origins.

What kind of scattering processes may contribute to the LDOS? We assume that the following processes are important: (i) out-of-plane scattering into the 3D free space, (ii) in-plane scattering into the surrounding PCS cladding, (iii) backward scattering into the backward propagating mode, and (iv) intermode scattering into other waveguide modes. As described above, a simple v_g -scaling corresponds to (i) only. Thus, the above findings suggest that we should certainly consider other scattering processes. In addition, we assume that the waveguide disorder mainly originates during the lithographic patterning, and thus we take only *in-plane* disorder into account (this is not a model requirement). In other words, we assume that the disorder does not destroy the vertical symmetry; if it does, polarization-mixing scattering would occur, and this assumption is supported by Fig. 1(a).

First we consider the region labeled *A* in Fig. 2(b) for W1. Since region *A* is purely a single-mode region, the only possible scattering process other than out-of-plane scattering is backscattering. Theoretically,¹² the backward scattering loss scales as $(1/v_g)^2$, which can be intuitively understood because the LDOS of the final state is the LDOS of the propagating mode, proportional to $1/v_g$. With this model in mind, we plot $L(\omega)v_g^2$ in Fig. 3(a). In contrast to the previous $L(\omega)v_g$ plot, this value is almost constant in the vicinity of the mode edge, which proves the $(1/v_g)^2$ scaling for the propagation loss. This directly confirms that when v_g becomes small, the backward scattering—which has not been carefully studied with respect to PCS waveguides—becomes important (and indeed dominant). To our knowledge, this is the first experimental verification of $(1/v_g)^2$ scaling in PCS waveguides and particularly important for the practical realization of ultraslow light within PCS waveguides.

Second, we examine the region labeled *B* for W1. There is an odd mode in region *B* at the same frequency, and thus intermode scattering into this odd mode is possible. Since

this odd mode is partly located above the light line, intermode scattering ultimately leads to radiation loss. In Fig. 2(b), the loss apparently increases in the presence of the odd mode. In addition, there is a structure indicating loss peak at around 0.284 in region *B* in Fig. 2(b), which seems to correspond to the edge of the odd mode (that is, the peak in the LDOS of the odd mode). Though the peak is not distinct, we observed similar peak structures for all samples we measured. Such peak structures can also be observed in the calculated $\text{Im}[G]$ spectrum in Fig. 4(a), too. We believe that the peaks near $\omega=0.286$, 0.290, and 0.296 may correspond to the lower mode edge ($k=0.5$), the upper mode edge ($k=0$), and the maximum point ($k\sim 0.3$) of the odd mode, respectively. We have confirmed that the $\text{Im}[G]$ in region *B* has different spatial symmetry from that in region *A*, proving that the odd mode is the dominant contribution to scattering.

Next, we examine the loss spectrum for W0.7 shown in Fig. 2(c). W0.7 has a fundamentally different dispersion from W1.0: It has two mode-gap cutoffs and while there is no odd mode, there is a double-mode region. Figure 4(b) shows the calculated $\text{Im}[G]$ spectrum for W0.7. In Fig. 2(c), we again define *A* as the single-mode region and *B* as the double-mode region [see Fig. 1(d)]. Region *A* can be explained in a similar way to W1.0.¹⁴ We also observe a large loss increase in region *B*. The loss increase in the lower part of region *B* is attributed to the intermode scattering into the small- k mode for $\omega>0.277$, which is located above the light line; the increase in the upper part of region *B* corresponds to a decrease in v_g . We believe the loss peak in Fig. 2(c) and the $\text{Im}[G]$ peak near 0.278 in Fig. 4(b) may correspond to the mode edge of the small- k mode [$\omega=0.276$ in Fig. 1(d)] and that the rapid loss increase above $\omega=0.28$ in Fig. 2(c) and the peak of $\text{Im}[G]$ near $\omega=0.285$ in Fig. 4(b) corresponds to the maximum point ($k\sim 0.25$) [$\omega=0.287$ in Fig. 1(d)]. Note the influence from the light line ($\omega>0.286$) may coexist, but this is difficult to distinguish at this experimental resolution.

In the above, we have succeeded in qualitatively explaining the observed loss spectral structures in terms of possible scattering processes in PCS waveguides. Since all of these processes are included in G , we can *quantitatively* calculate the loss spectrum by the GFT method. For this we need information on the disorder that is described by the σ and the correlation length l_c of $\Delta\epsilon$ (defined as the spatial correlation of the permittivity disorder $\langle\Delta\epsilon(\mathbf{r})\Delta\epsilon(\mathbf{r}')\rangle$).¹² We employ 3 and 40 nm for σ and l_c , respectively. While the σ value was determined from the SEM images as described before, it was difficult to experimentally determine l_c so we chose an l_c of 40 nm to fit our experimental data. We regard this value to be physically reasonable because it was reported that straight nanoscale waveguides show an in-plane correlation length of ~ 50 nm.¹⁵ Also, a change of σ and l_c does not change the loss spectrum shape (only a shift in the absolute loss value occurs), and thus we can quantitatively compare the calculated loss spectrum shape with the measured one. The calculated loss data, including all scattering mechanisms, are plotted by circles in Figs. 2(b) and 2(c). We observe a very good agreement in terms of spectral shape for W1 and W0.7. This shows that our model including backscattering and intermode scattering processes successfully explains the observed

loss spectra. This agreement also supports our hypothesis that the observed loss is mainly determined by the in-plane disorder. In Fig. 3(b), we plot the calculated $L(\omega)v_g$ and calculated $L(\omega)v_g^2$ for W1 in a similar way to the measured results in Fig. 3(a). The calculated and measured data are clearly very similar. From this agreement, as regards the $(1/v_g)^2$ scaling near the mode-gap cutoff, the dominant contribution of the backscattering process is unambiguously confirmed. Note that this enhanced backscattering is primarily due to low v_g , and not due to the high dispersion in the vicinity of the gap edge. Thus, we expect the similar behavior would occur for any slow light modes. Finally, we stress again that no changes in structural parameters are needed to fit both waveguides.

Before closing, we consider the effect of the in-plane radiation process, which we have not yet considered in our discussion, namely the scattering into the surrounding PCS cladding. It has sometimes been argued that the existence of the PBG can reduce the propagation loss due to the reduction of the LDOS of the final state.¹⁶ In the W0.7 sample, the PBG edge for the surrounding bulk region is located at $\omega = 0.2623$, which is inside the transmission window. We observe that the loss does not increase noticeably below this frequency that indicates that the reduction is not very great. We assume that the LDOS reduction inside the 2D plane is negligible compared with the LDOS of the effective-medium 3D space. Such suppression could be substantial for 3D but

not for 2D PBG waveguides. Moreover, we observed interesting loss peaks near the PBG edge as shown in Fig. 2(c). In fact, this loss varied from sample to sample, but almost always exists close to the PBG edge for most samples. Considering that the LDOS of the PCS cladding becomes significantly large near the PBG edge, we believe that this peak comes from the in-plane scattering into the PBG cladding. This means that the in-plane scattering is only visible in the vicinity of PBG edges.

In summary, we have measured the broadband propagation loss spectra of record low loss PCS waveguides. The measured loss spectra exhibited complicated ω dependence, which is drastically different to a simple $1/v_g$ scaling picture. We have successfully clarified the underlying physical processes that cause disorder-induced scattering in PCS by comparing with a photon GFT theory. The underlying physical features of the loss spectra are found to be fundamentally different from those of conventional optical waveguides, and should be seriously considered when attempting to obtain better PCS waveguides. Moreover, for slow light modes, scattering loss is found to scale inversely with the squared group velocity as was predicted recently by theory.

We would like to thank T. Tamamura and D. Takagi for sample fabrication, and J. E. Sipe and Jeff. F. Young for useful discussions.

*Electronic address: kuramoti@nttbl.jp

[†]Present address: Department of Physics, Queen's University, Kingston, Ontario K7L 3N6, Canada.

¹S. G. Johnson, P. R. Villeneuve, S. Fan, and J. D. Joannopoulos, *Phys. Rev. B* **62**, 8212 (2000).

²M. Lončar, D. Nedeljković, T. Doll, J. Vučković, A. Scherer, and T. P. Pearsall, *Appl. Phys. Lett.* **77**, 1937 (2000).

³M. Notomi, K. Yamada, A. Shinya, J. Takahashi, C. Takahashi, and I. Yokohama, *Phys. Rev. Lett.* **87**, 253902 (2001).

⁴C. J. M. Smith, H. Benisty, S. Olivier, M. Rattier, C. Weisbuch, T. F. Krauss, R. M. De La Rue, R. Houdré, and U. Oesterle, *Appl. Phys. Lett.* **77**, 2813 (2000).

⁵M. Notomi, K. Yamada, J. Takahashi, C. Takahashi, and I. Yokohama, *Electron. Lett.* **37**, 243 (2001).

⁶M. Notomi, A. Shinya, K. Yamada, J. Takahashi, C. Takahashi, and I. Yokohama, *IEEE J. Quantum Electron.* **38**, 736 (2002).

⁷S. J. McNab, N. Moll, and Y. A. Vlasov, *Opt. Express* **11**, 2927 (2003).

⁸Y. Sugimoto, Y. Tanaka, N. Ikeda, Y. Nakamura, K. Asakawa, and K. Inoue, *Opt. Express* **12**, 1090 (2004).

⁹M. Notomi, A. Shinya, S. Mitsugi, E. Kuramochi and H.-Y. Ryu, *Opt. Express* **12**, 1551 (2004).

¹⁰D. Marcuse, *Theory of Dielectric Waveguides* (Academic, New York, 1974).

¹¹Y. Tanaka, Y. Sugimoto, N. Ikeda, H. Nakamura, K. Asakawa, K. Inoue, and S. G. Johnson, *Electron. Lett.* **40**, 174 (2004).

¹²S. Hughes, L. Ramunno, J. F. Young, and J. E. Sipe, *Phys. Rev. Lett.* **94**, 033903 (2005); International Quantum Electronics Conference (CLEO/IQEC), ITHL5 San Francisco, CA, 2004 (unpublished).

¹³K. Sakoda, *Optical Properties of Photonic Crystals* (Springer Verlag, Berlin, 2001).

¹⁴We do not discuss here the difference between the absolute loss values of W1.0 and W0.7, but the small v_g and large field intensity near the air-Si interface for W0.7 will lead to greater loss.

¹⁵K. K. Lee, D. R. Lim, H.-C. Luan, A. Agarwal, J. Foresi, and L. C. Kimerling, *Appl. Phys. Lett.* **77**, 1617 (2000).

¹⁶M. L. Povinelli, S. G. Johnson, E. Lidorikis, J. D. Joannopoulos, and M. Soljačić, *Appl. Phys. Lett.* **84**, 3639 (2004).